Magnetic correlations in martensitic Ni-Mn-based Heusler shape-memory alloys: Neutron polarization analysis

S. Aksoy and M. Acet
Experimentalphysik, Universität Duisburg-Essen, D-47048 Duisburg, Germany

P. P. Deen
Institut Laue-Langevin, BP 156, 38042 Grenoble Cedex 9, France

L. Mañosa and A. Planes
Departament d'Estructura i Constituents de la Matèria, Facultat de Física, Universitat de Barcelona, Diagonal 647, E-08028 Barcelona, Catalonia, Spain

(Received 9 December 2008; revised manuscript received 21 April 2009; published 3 June 2009)

In ferromagnetic Ni-Mn-based Heusler alloys undergoing martensitic transformations, a sudden drop in the magnetization is observed as the temperature decreases through the martensitic-transformation temperature M_s. To understand the cause of the drop and thereby the nature of the magnetic coupling in this temperature region, we carry out neutron-polarization-analysis experiments on two prototypes, $Ni_{50}Mn_{40}Sb_{10}$ and $Ni_{50}Mn_{37}Sn_{13}$. We show that in the vicinity of M_s, the magnetic correlations at temperatures $T<M_s$ are antiferromagnetic, whereas they are ferromagnetic above M_s and well beyond the Curie temperature of the austenitic state.

DOI: 10.1103/PhysRevB.79.212401 PACS number(s): 75.30.Cr, 75.50.−y, 75.60.Ej

Ni-Mn-based ferromagnetic (FM) Heusler alloys undergoing martensitic transformations have become the focus of intensive research related to magnetic-field-induced structural modifications[1] and magnetocaloric effects[2] since the discovery of the magnetic shape-memory effect in Ni-Mn-Ga.[3] Presently, much work is invested in studies aimed at producing working prototypes of magnetic-field-actuated devices[4,5] as well as understanding how magnetic properties and the martensitic transformation are interrelated.[6–10]

A common feature to all Ni-Mn-based Heusler alloys undergoing a martensitic transformation is that in small magnetic fields of about 10 mT or less, all systems show a drop in the temperature dependence of the magnetization $M(T)$ at the transformation start temperature M_s.[11,12] In fact, in substantially higher measuring fields of about 5 T, the drop persists, except in Ni-Mn-Ga alloys where the change in $M(T)$ between the two states at M_s reverses sign above a certain field.[13] The cause of the drop in $M(T)$ in Ni-Mn-based Heusler alloys is often thought to be related to the development of local antiferromagnetic (AF) ordering associated with changing distance of the Mn-Mn bonding.[9] Indirect evidence for the presence of such possible states is provided by associating them to the nonsaturating behavior of the magnetic-field dependence of the magnetization $M(H)$ at $T<M_s$.[11,12] More recently, the observation of exchange bias at low temperatures in Ni-Mn-based Heusler alloys has further strengthened the thesis of the presence of AF components,[14–17] whereas results of Mössbauer experiments[18] suggest the presence of a paramagnetic (PM) state below M_s.

Since understanding magnetic shape-memory and magnetocaloric effects exhibited by these materials is closely related to the understanding of the details of the magnetoelastic properties at martensitic transformations, we have undertaken a study to resolve the nature of the magnetic interactions in the martensitic and austenitic states. For this purpose, we have carried out neutron-polarization analysis on two prototypical systems, $Ni_{50}Mn_{40}Sb_{10}$ (no FM ordering in the austenitic state) and $Ni_{50}Mn_{37}Sn_{13}$ (presence of FM ordering in the austenitic state). We determine first the structural- and magnetic-transition temperatures of the samples used in the experiments and characterize their magnetic properties by conventional magnetization-measurement techniques. We use samples from the same batch for the polarization-analysis experiments. The details of the characterizations are presented in Fig. 1.

$Ni_{50}Mn_{37}Sn_{13}$ orders ferromagnetically in the austenitic

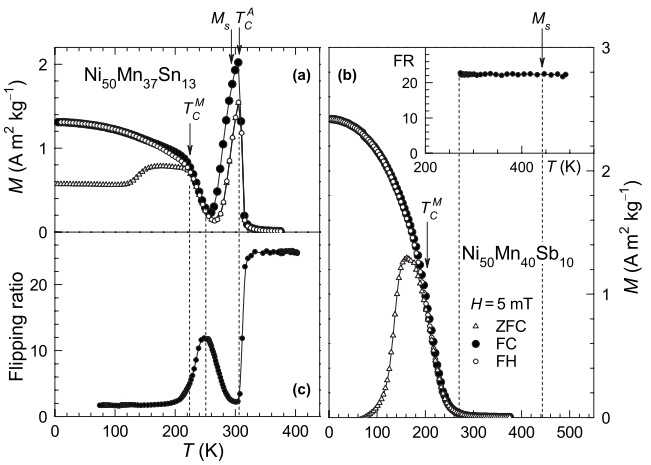

FIG. 1. Characterization of the samples for the polarization analysis experiments of $Ni_{50}Mn_{37}Sn_{13}$ and $Ni_{50}Mn_{40}Sb_{10}$. (a) $M(T)$ in the ZFC, FC, and FH states for $Ni_{50}Mn_{37}Sn_{13}$. (b) $M(T)$ in the ZFC, FC, and FH states for $Ni_{50}Mn_{40}Sb_{10}$. (c) $R_F(T)$ for $Ni_{50}Mn_{37}Sn_{13}$. The inset in part (b) shows $R_F(T)$ for $Ni_{50}Mn_{40}Sb_{10}$. The dashed lines relate the temperature positions of the extrema to $M(T)$ in part (a) and the temperature positions of M_s and the lowest temperature of R_F to $M(T)$ in part (b).

state at $T_C^A = 310$ K [Fig. 1(a)]. Just below this temperature, the sample undergoes a martensitic transformation at $M_s \approx 305$ K, and the magnetization practically vanishes as the temperature drops. At a lower temperature $T_C^M \approx 220$ K, the sample orders ferromagnetically again. This sample serves as a prototype for Ni-Mn-based Heusler systems for which the austenitic state is FM and the magnetization rapidly drops below M_s.

In $Ni_{50}Mn_{40}Sb_{10}$ the structural transformation takes place from a PM austenitic state to a PM martensitic state at about $M_s = 440$ K determined from calorimetric measurements (not shown here). This sample orders ferromagnetically in the martensitic state at a Curie temperature $T_C^M \approx 210$ K as seen in Fig. 1(b), where $M(T)$ is plotted for the zero-field-cooled (ZFC), field-cooled (FC), and field-heated (FH) states. There is no FM ordering in the austenitic state of this sample.

Polarization-analysis experiments were carried out on annealed 10 μm powder samples (about 3 g) on the D7 diffuse-scattering spectrometer at the Institut Laue-Langevin, Grenoble using 4.86 Å incident neutrons. This multidetector instrument allows full *XYZ*-polarization analysis to separate the nuclear-coherent, magnetic, and spin-incoherent cross sections, $(d\sigma/d\Omega)_{\text{nuc}}$, $(d\sigma/d\Omega)_{\text{mag}}$, and $(d\sigma/d\Omega)_{\text{inc}}$, solely from geometrical-scattering conditions.[19,20] The cross sections are corrected for detector efficiency via a vanadium sample, and the analyzer efficiency is corrected via a quartz sample. The absolute cross sections can be determined via comparative scattering of a vanadium sample. Further powder-diffraction experiments with neutron wavelength 1.594 Å on $Ni_{50}Mn_{37}Sn_{13}$ were carried out on the D2B spectrometer at the same institute.

In addition to diffraction cross sections, the flipping ratio (R_F) of the neutrons traversing the sample is measured. R_F is defined as the ratio of the spin-up to spin-down eigenstates and is a measure of the neutron depolarization. In a sample where the net magnetization is zero, the neutron-polarization state and thus the R_F are not affected by the sample. However, in a sample with FM domains, a neutron spin will experience a torque causing it to precess around the magnetization direction of the FM domains that are inhomogeneously distributed across the beam profile. This causes a nonadiabatic depolarization of the neutron state with a resultant drop in R_F. The depolarization measurement is therefore a very sensitive tool for the determination of ferromagnetic-domain formation.

For the $Ni_{50}Mn_{40}Sb_{10}$ sample, M_s separates PM-austenitic and PM-martensitic states and $R_F \approx 23$, which remains temperature independent from the highest temperatures down to temperatures approaching T_C^M, as shown in the inset of Fig. 1(b).

$R_F(T)$ for $Ni_{50}Mn_{37}Sn_{13}$ is shown in Fig. 1(c). At high temperatures, well in the PM state, $R_F \approx 25$. The initial sharp drop with decreasing temperature in $R_F(T)$ is related to the onset of FM order below T_C^A, whereby the beam is depolarized by the FM domains. However, just below M_s, R_F begins to recover and increases with decreasing temperature as the amount of FM austenite decreases. It then runs through a local maximum of $R_F \approx 12$ at a temperature corresponding to the local minimum in $M(T)$. R_F does not regain its maximum value of 25 because some rest austenite remains at these

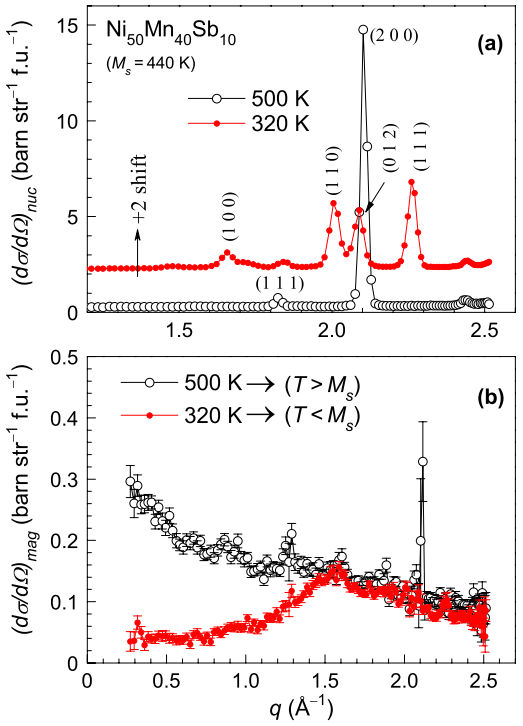

FIG. 2. (Color online) q dependence of the neutron-scattering cross sections in the austenitic (500 K) and martensitic (320 K) states of $Ni_{50}Mn_{40}Sb_{10}$ ($M_s = 440$ K). (a) The nuclear cross section plotted in the range $1.2 \leq q \leq 2.6$ Å^{-1}. No reflections are found at lower q in either data. Open circles $L2_1$ (indexed horizontally) and filled circles 4O (indexed vertically). The data for 320 K are shifted vertically by +2 units for clarity. (b) The magnetic cross section. The forward scattering present in the austenitic state (500 K) vanishes in the martensitic state (320 K).

temperatures. As the temperature further decreases, so does $R_F(T)$, whereby the decrease progresses over a relatively broad temperature range from about 250 to 200 K as opposed to the sharper decrease found around T_C^A. This is an indication that the position of T_C^M is not well defined. The broad nature of the FM transition in the martensitic state is also identified in $M(T)$ in Figs. 1(a) and 1(b). When measured in a small external magnetic field as 5 mT, $M(T)$ for a ferromagnet would be expected to rise sharply at the Curie temperature to a value corresponding to the demagnetization limit and then run relatively temperature independent as the temperature decreases.[11] Here we see that this is not the case for $M(T)$ below T_C^M for either sample.

We first focus on the results of the polarization analysis experiments on $Ni_{50}Mn_{40}Sb_{10}$ shown in Fig. 2. $(d\sigma/d\Omega)_{\text{nuc}}$ vs q plotted in Fig. 2(a) shows diffraction patterns at 320 and 500 K related to the martensitic structure and to the cubic Heusler phase, respectively. The data for 320 K are shifted vertically by +2 units for clarity. From these data, the martensitic structure is determined as 4O modulated, in agreement with earlier studies.[21] $(d\sigma/d\Omega)_{\text{mag}}$ vs q plotted in Fig. 2(b) features substantial scattering at low q values, even at temperatures as high as 500 K, indicating the presence of FM correlations although no FM ordering in the austenitic state is found in this sample. The narrow peak in the magnetic

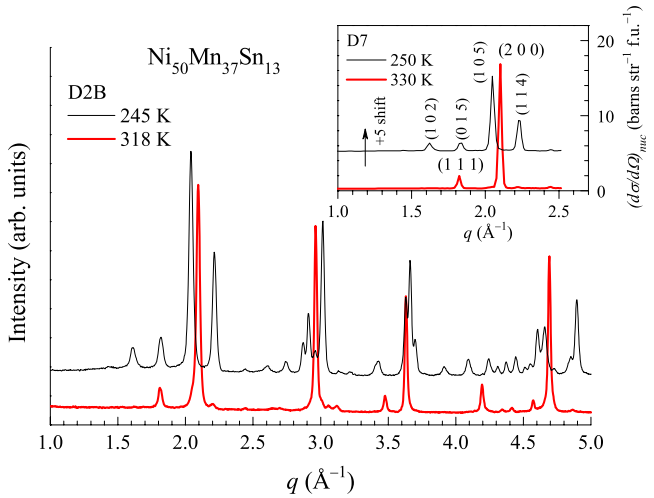

FIG. 3. (Color online) The q dependence of the neutron-diffraction spectrum of $Ni_{50}Mn_{37}Sn_{13}$ obtained on the D2B spectrometer at 245 K (fine line, black) and 318 K (heavy line, red). The inset shows the nuclear cross section in the austenitic (330 K) and martensitic (250 K) states obtained on the D7 spectrometer. The data for 250 K are shifted vertically by +5 units for clarity. The structure in the martensitic state is $10M$ modulated (austenite indexed horizontally and martensite indexed vertically).

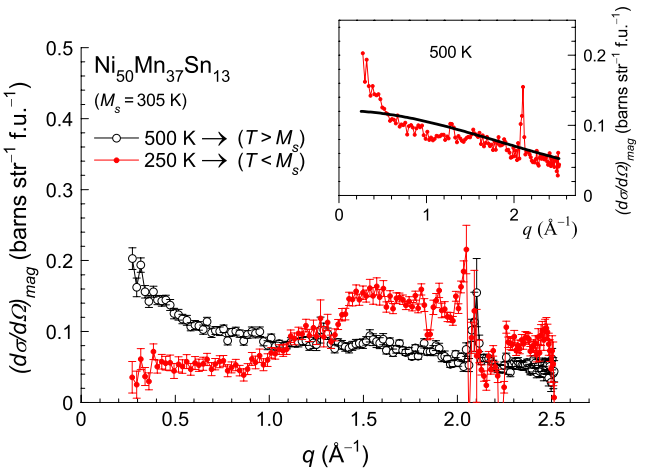

FIG. 4. (Color online) The q dependence of the magnetic cross section at 500 and 250 K for $Ni_{50}Mn_{37}Sn_{13}$. The forward scattering present in the austenitic state essentially vanishes in the martensitic state (M_s=305 K). The inset shows the comparison of the magnetic cross section at 250 K and the q dependence of the Mn form factor (heavy line) normalized to the value $(d\sigma/d\Omega)_{mag}$ at q=1.5 Å^{-1}.

scattering at 500 K accompanied by relatively large error bars at $q \approx 2.1$ Å^{-1} results most probably from systematic errors arising from the separation of nuclear and magnetic contributions to the scattering, as this position corresponds to that of the (200) peak in Fig. 2(a). At 320 K, which corresponds to a temperature well within the martensitic state, the scattering at low q is very weak indicating that FM correlations have practically vanished. However, strong and broad diffuse scattering still remains above about 0.8 Å^{-1} up to the highest q values measured. This broad diffuse scattering is expected to be due to the presence of AF correlations.

Next we examine the results for $Ni_{50}Mn_{37}Sn_{13}$. Powder diffraction patterns taken on the D2B spectrometer at 245 ($T<M_s$) and 318 K ($T>M_s$) are shown in Fig. 3. In the low-symmetry martensitic state, the reflections associated with the high-symmetry austenitic cubic phase are split into a multitude of reflections at various zones from which the $10M$ modulated structure can be identified in agreement with earlier studies.[11] We use these data in the discussions given below to account for the presence of AF correlations in Ni-Mn-based martensitic Heusler systems. The inset in the figure shows $(d\sigma/d\Omega)_{nuc}$ vs q at similar temperatures resulting from polarization-analysis data taken on the D7 spectrometer. The data in the inset for 250 K are shifted vertically by +5 units for clarity. Data from both spectrometers agree well. On the D7 spectrometer, the full XYZ-polarization-analysis technique was employed at 500 K, whereas at 250 K, only Z polarization was employed because of the lower value of $R_F \approx 12$ at this temperature with respect to the base $R_F \approx 25$ of the instrument. This arises due to the possible presence of residual ferromagnetic austenite. Since the analyzers are setup to count only non-spin-flip neutrons in the Z direction, using the XYZ method at low R_F and in the presence of residual ferromagnetic austenite would give rise to uncertainties in the scattering information when the neutron spin is rotated into the X-Y plane and, therefore, this method was not employed. Nevertheless, the beam polarization at 250 K is still sufficiently high to apply Z-polarization analysis [Fig. 1(c)]. The data are corrected for the flipping ratio. Furthermore, assuming that the $(d\sigma/d\Omega)_{inc}$ is temperature independent, the q dependence of $(d\sigma/d\Omega)_{mag}$ at 250 K can be evaluated by using the q dependence of $(d\sigma/d\Omega)_{inc}$ at 500 K which was obtained using the XYZ method (see examples in Ref. 20).

$(d\sigma/d\Omega)_{mag}$ vs q for $Ni_{50}Mn_{37}Sn_{13}$ obtained at 250 and 500 K is shown in Fig. 4. The magnetic scattering profile at 500 K is similar to that of $Ni_{50}Mn_{40}Sb_{10}$ for the same temperature (Fig. 2). At this temperature, there is substantial forward scattering indicating the presence of FM correlations. In the martensitic state at 250 K, which corresponds nearly to the temperature at which $M(T)$ shows a minimum and $R_F(T)$ shows a local maximum, the q dependence of $(d\sigma/d\Omega)_{mag}$ is similar to that of $Ni_{50}Mn_{40}Sb_{10}$. Namely, the FM correlations vanish and AF correlations occur. The relatively large scattering in the data around q=2.1 Å^{-1} [corresponding to the (200) Bragg position in the austenitic state] is most probably related to the presence of FM rest austenite that causes partial depolarization of the beam and leads to uncertainties in determining $(d\sigma/d\Omega)_{mag}$ at these q values and to systematic errors arising from the separation of nuclear and magnetic contributions, as in the case in Fig. 2(b). The inset compares the q dependence of the magnetic cross section at 250 K to that of the single-ion Mn form factor normalized to the value $(d\sigma/d\Omega)_{mag}$ at q=1.5 Å^{-1}. The q dependence of the form factor represents noncorrelated behavior. The different behaviors of the q dependencies of the obtained data and the form factor, especially at low-q values, point out further that the scattering at low q is related to FM correlations.

In both Figs. 2(b) and 4 the low-temperature data exhibit a broad shoulder beginning at about q=0.8 Å^{-1} and extend-

ing to above the highest q value of 2.5 Å^{-1} accessible on the D7 spectrometer. The scattering profiles are peaked nearly at the same value of about $q=1.6$ Å^{-1}. In Fig. 3, one sees that this q range encompasses the half-q positions of the multitude of Bragg reflections appearing between about $q=1.5$ Å^{-1} and above $q=5.0$ Å^{-1} (Fig. 3). Due to the primarily doubled AF unit cell with respect to the crystallographic unit cell, AF correlations would be observed as weak broad peaks centered at half-q positions of the various crystallographic zones. However, due to the multitude of reflections associated with the martensitic state, such peaks overlap to form the observed broad shoulder. Therefore, a meaningful correlation length cannot be extracted from the data. Such AF correlations exhibiting similar spectra have been previously observed in, e.g., YMn_2 where diffuse-scattering centered at half-Bragg positions develops into a single broad diffuse peak.[22–24]

The data presented above show that FM correlations are present at $T>M_s$ and for their presence, long-range magnetic ordering does not necessarily have to occur at a lower temperature in the austenitic state, as in the case of $Ni_{50}Mn_{40}Sb_{10}$, or it may occur well above T_C^A, as in the case of $Ni_{50}Mn_{37}Sn_{13}$. Because of the smaller cell volume and therefore the smaller Mn-Mn separation in the modulated martensitic state with respect to the cubic austenitic state in these systems,[7] FM exchange can be expected to weaken below M_s. Indeed, the data show this directly as the vanishing of FM correlations just below M_s and the concurrent appearance of AF correlations. This is also accompanied by a loss in the intensity in the magnetic scattering, particularly for $Ni_{50}Mn_{40}Sb_{10}$, which would correspond to a decrease in the magnetic moment. However, because of the low incident energy of the neutrons in the present experiments, integration of the magnetic scattering over the Brillouin zone does not allow an exact determination of the magnetic moment in the austenitic and martensitic states.

One can additionally relate the present observations to properties featured by Ni-Mn-based Heusler alloys in various other experiments: the cause of the strong splitting of the FC and ZFC branches in $M(T)$ [Figs. 1(b) and 1(c)], the "smeared" nature of the progress of FM ordering below T_C^M, as well as the more recently observed exchange-bias effects at low temperatures in Ni-Mn-based martensitic Heusler alloys,[14,15] all being related to the presence of AF exchange, is justified with the results of the present experiments.

This work was supported by Deutsche Forschungsgemeinschaft (Grant No. SPP1239), CICyT (Spain) (Project No. MAT2007-61200), and ILL-Grenoble.

[1] R. Kainuma, Y. Imano, W. Ito, Y. Sutou, H. Morito, S. Okamoto, O. Kitakami, K. Oikawa, A. Fujita, T. Kanomata, and K. Ishida, Nature (London) **439**, 957 (2006).
[2] T. Krenke, E. Duman, M. Acet, E. F. Wassermann, X. Moya, L. Mañosa, and A. Planes, Nature Mater. **4**, 450 (2005).
[3] K. Ullakko, J. K. Huang, C. Kantner, R. C. O'Handley, and V. V. Kokorin, Appl. Phys. Lett. **69**, 1966 (1996).
[4] F. Khelfaoui, M. Kohl, J. Buschbeck, O. Heczko, S. Fähler, and L. Schultz, Eur. Phys. J. Spec. Top. **158**, 167 (2008).
[5] U. Gaitzsch, M. Pötschke, S. Roth, B. Rellinghaus, and L. Schultz, Scr. Mater. **57**, 493 (2007).
[6] T. Krenke, E. Duman, M. Acet, and E. F. Wassermann, Xavier Moya, Lluís Mañosa, Antoni Planes, E. Suard, and B. Ouladdiaf, Phys. Rev. B **75**, 104414 (2007).
[7] S. Aksoy, T. Krenke, M. Acet, E. F. Wassermann, X. Moya, L. Mañosa, and A. Planes, Appl. Phys. Lett. **91**, 251915 (2007).
[8] L. Mañosa, X. Moya, A. Planes, O. Gutfleisch, J. Lyubina, M. Barrio, J.-L. Tamarit, S. Aksoy, T. Krenke, and M. Acet, Appl. Phys. Lett. **92**, 012515 (2008).
[9] P. J. Brown, A. P. Gandy, K. Ishida, R. Kainuma, T. Kanomata, K. U. Neumann, K. Oikawa, B. Ouladdiaf, and K. R. A. Ziebeck, J. Phys.: Condens. Matter **18**, 2249 (2006).
[10] P. A. Bhobe, K. R. Priolkar, and P. R. Sarode, J. Phys. D **41**, 045004 (2008).
[11] T. Krenke, M. Acet, E. F. Wassermann, X. Moya, L. Mañosa, and A. Planes, Phys. Rev. B **72**, 014412 (2005).
[12] T. Krenke, M. Acet, E. F. Wassermann, X. Moya, L. Mañosa, and A. Planes, Phys. Rev. B **73**, 174413 (2006).
[13] J. Marcos, L. Mañosa, A. Planes, F. Casanova, X. Batlle, and A. Labarta, Phys. Rev. B **68**, 094401 (2003).
[14] Z. Li, C. Jing, J. Chen, S. Yuan, S. Cao, and J. Zhang, Appl. Phys. Lett. **91**, 112505 (2007).
[15] M. Khan, I. Dubenko, S. Stadler, and N. Ali, Appl. Phys. Lett. **91**, 072510 (2007).
[16] M. Khan, I. Dubenko, S. Stadler, and N. Ali, J. Appl. Phys. **102**, 113914 (2007).
[17] M. Khan, I. Dubenko, S. Stadler, and N. Ali, J. Phys.: Condens. Matter **20**, 235204 (2008).
[18] R. Y. Umetsu, R. Kainuma, Y. Amako, Y. Taniguchi, T. Kanomata, K. Fukushima, A. Fujita, K. Oikawa, and K. Ishida, Appl. Phys. Lett. **93**, 042509 (2008).
[19] O. Schärpf and H. Capellmann, Phys. Status Solidi A **135**, 359 (1993).
[20] J. R. Stewart, P. P. Deen, K. H. Andersen, H. Schober, J.-F. Barthélémy, J. M. Hillier, A. P. Murani, T. Hayes, and B. Lindenau, J. Appl. Crystallogr. **42**, 69 (2009).
[21] Y. Sutou, Y. Imano, N. Koeda, T. Omori, R. Kainuma, K. Ishida, and K. Oikawa, Appl. Phys. Lett. **85**, 4358 (2004).
[22] J. Deportes, B. Ouladdiaf, and K. R. A. Ziebeck, J. Phys. (Paris) **48**, 1029 (1987).
[23] M. Shiga, H. Wada, Y. Nakamura, J. Deportes, B. Ouladdiaf, and K. R. A. Ziebeck, J. Phys. Soc. Jpn. **57**, 3141 (1988).
[24] T. Freltoft, P. Böni, G. Shirane, and K. Motoya, Phys. Rev. B **37**, 3454 (1988).